Chapter 1
Introduction to Synchrotron Radiation

Antonella Balerna and Settimio Mobilio

Abstract Relativistic charged particles forced to move along curved trajectories by applied magnetic fields emit electromagnetic radiation called Synchrotron Radiation; today electron storage rings are routinely used to provide synchrotron radiation to users in a wide spectral range from infrared to hard X-rays. Thanks to its peculiar characteristics, synchrotron radiation is one of the more powerful tools for investigating the properties of matter in many different fields like molecular and atomic physics, cell biology, medical applications, nanotechnology, catalysis and cultural heritage. Up to now three generations of synchrotron radiation sources emitting radiation with increasing quality have been developed; the fourth generation, based on free-electron lasers, already produces high power and ultrafast pulses of highly coherent radiation. In the present contribution, the main characteristics and properties of the synchrotron radiation sources and of the produced radiation are introduced and explained using a simple approach.

1.1 Introduction

When electrons or other charged particles moving at relativistic speeds are forced by magnetic fields to follow curved trajectories they emit electromagnetic radiation in the direction of their motion, known as synchrotron radiation. Synchrotron radiation is emitted, for example, by cosmic sources. The blue light visible in Fig. 1.1, that shows a mosaic image of the Crab Nebula, the remnant of a supernova explosion seen on earth by many astronomers in 1054, comes from high energy electrons whirling

A. Balerna (✉)
Laboratori Nazionali di Frascati, INFN, via E. Fermi 40, 00044 Frascati, RM, Italy
e-mail: balerna@lnf.infn.it

S. Mobilio
Dipartimento di Scienze, Universita' Roma Tre, via della Vasca Navale 84, 00146 Rome, Italy
e-mail: settimio.mobilio@uniroma3.it

S. Mobilio et al. (eds.), *Synchrotron Radiation*,
DOI: 10.1007/978-3-642-55315-8_1, © Springer-Verlag Berlin Heidelberg 2015

Fig. 1.1 NASA Hubble Space Telescope image of the Crab Nebula (*NASA, ESA and Allison Loll/Jeff Hester (Arizona State University). Acknowledgement: Davide De Martin (ESA/Hubble)*)

around magnetic field lines due to the presence of a pulsar (pulsating radio source). In this lecture we present the properties and characteristics of the synchrotron radiation produced in particle accelerators by electrons or positrons; such radiation is extremely intense and extends over a broad energy range from the infrared through the visible and ultraviolet, into the soft and hard x-ray regions of the electromagnetic spectrum. It was observed for the first time in 1947 at the General Electric synchrotron in the USA; for a long time it was considered only as a problem for particle physics since represents the major source of energy loss in high energy particle accelerators. Only in the late sixties it was realized that synchrotron radiation was very useful for condensed matter research. Since then, there was an explosive growth in its use and dedicated synchrotron radiation facilities were built, making this radiation a unique tool in many research fields. Nowadays synchrotron radiation is being used to study many aspects of the structure of matter at the atomic and molecular scale, from surface properties of solids to the structure of protein molecules.

1.2 Storage Rings and Synchrotron Radiation Sources

Electrons traveling at a speed close to c, the speed of light, and forced to change the direction of their motion under the effect of magnetic fields (perpendicular to the direction of their motion), emit light, with peculiar characteristics, known as synchrotron radiation. The 'natural' man-made sources of this radiation [1] are high energy, electron or positron circular accelerators, like storage rings. They consist

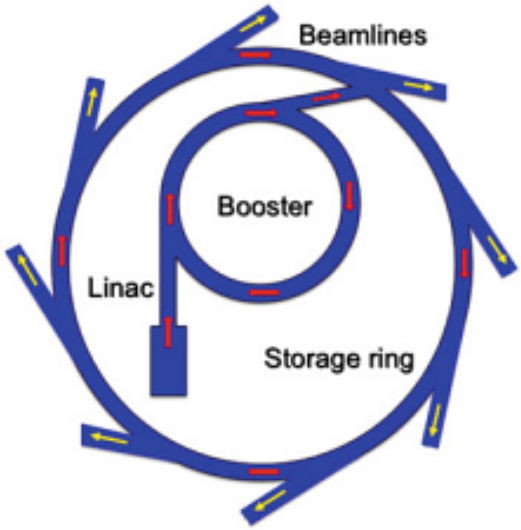

Fig. 1.2 Schematic planar view of a synchrotron radiation facility

of circular evacuated pipes where the electrons are forced to follow circular paths under the action of magnets placed along the circumference (bending magnets). The electrons enter the storage ring only after they have been accelerated by a linear accelerator or 'linac' until their energy reaches several millions of electron volts (MeV) and then by a booster ring that gives them a boost in energy from millions to billions or giga electron volts (GeV); at that point they are transferred to the final circular accelerator as shown in Fig. 1.2.

Here the electrons, if needed, may be further accelerated to higher energies by the radio frequency (RF) electric fields. When the electrons reach the expected energy they are in a quasi-stationary situation; forced to follow circular paths by the magnetic field of the bending magnets, they loose, during each turn, part of their energy, emitting synchrotron radiation. The energy lost in this way is fully regained in passing through the RF cavities. More precisely, storage rings consist of an array of magnets for focusing and bending the beam, connected by straight linear sections (see Fig. 1.3). In one or more of these linear sections, RF cavities are installed in order to accelerate the particles.

After its discovery in 1947, during the 1960s and early 70s pioneering use of the light was made in the so called *first generation synchrotron radiation facilities*; these machines were not dedicated to synchrotron radiation studies, but were used in a parasitic way, during high energy physics experiments. In the mid-70s facilities totally dedicated to synchrotron light, were built. These early-dedicated facilities, in which synchrotron light was mainly produced by bending magnets, are called *second generation sources*; also the use of high magnetic field devices, known as wigglers, started in this period. Afterwards, the optimization of magnetic structures, like wigglers and undulators, placed in straight sections made possible the realization of new synchrotron radiation sources the so called *third generation sources* like the European Synchrotron Radiation Facility (E.S.R.F. Grenoble France) and many other [2].

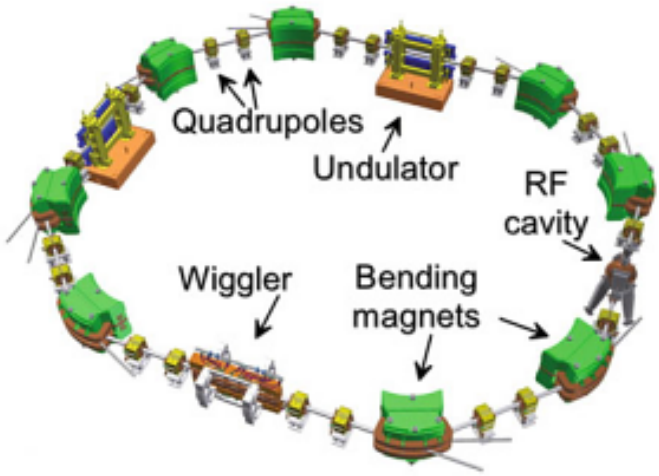

Fig. 1.3 Schematic view of a storage ring where some main elements like bending magnets, focusing and de-focusing magnets (quadrupoles), insertion devices (undulator, wigglers) and the RF (radio frequency) cavity are visible; the injection system is not shown (*courtesy of S. Tomassini INFN-LNF*)

Due to the advanced designs and beam control of third generation light sources, source size and divergence have been greatly improved. Nowadays for many experiments, like the ones involving imaging or microscopy, the beam has to be focused down to very small spots and so a relevant synchrotron radiation property becomes its spectral brightness[1] or flux per unit source area and per unit solid angle [3].

Undulators are excellent sources of high brightness radiation. This is shown in Fig. 1.4, where the gain in brightness achieved by the new synchrotron radiation sources, as a function of time, is shown; its increase of many orders of magnitude gives an idea of the spectacular progress obtained in beam quality by *third generation sources*.

While improvements in third generation synchrotron radiation sources are still possible, *fourth generation sources* are being developed, based on free electron lasers (FELs) able to produce very short coherent light pulses of very high peak intensity and brightness (FEL sources characteristics and applications are described in Chaps. 2 and 30).

[1] Brightness or brilliance? Several authors give different definitions while other authors use both terms to define the same quantity. The best thing to do, is to look to units to be sure of what you are dealing with. In any case in this lecture we will use the conclusions of [3] and define the spectral brightness as photons per second, per unit source size and divergence in a given bandwidth.

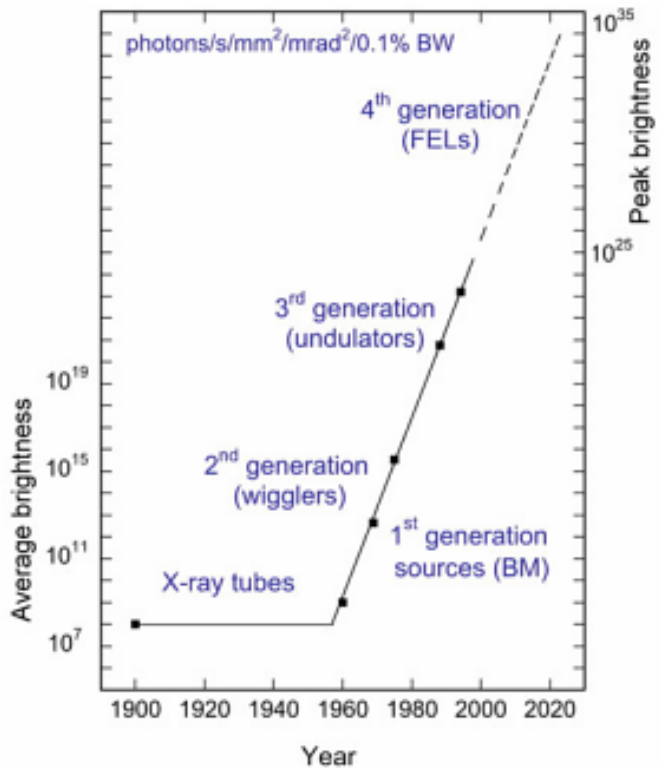

Fig. 1.4 Comparison between the average brightness of storage rings of different generations. As a comparison also the average brightness of x-ray tubes and of X-ray FELs (Free Electron Lasers) are reported (the figure was redrawn: it is based on data of Figs. 1.1 and 1.2 of [4])

Comparison of the brightness of different radiation sources at a given wavelength.

- 60 W light bulb

$$Brightness = 10^{6} \frac{Photons}{\mathrm{s} \cdot \mathrm{mm}^2 \cdot \mathrm{mr}^2 \cdot (0.1\,\%\,\mathrm{BW})}$$

- Sun

$$Brightness = 10^{10} \frac{Photons}{\mathrm{s} \cdot \mathrm{mm}^2 \cdot \mathrm{mr}^2 \cdot (0.1\,\%\,\mathrm{BW})}$$

- Third generation synchrotron radiation source: bending magnet

$$Brightness = 10^{16} \frac{Photons}{\mathrm{s} \cdot \mathrm{mm}^2 \cdot \mathrm{mr}^2 \cdot (0.1\,\%\,\mathrm{BW})}$$

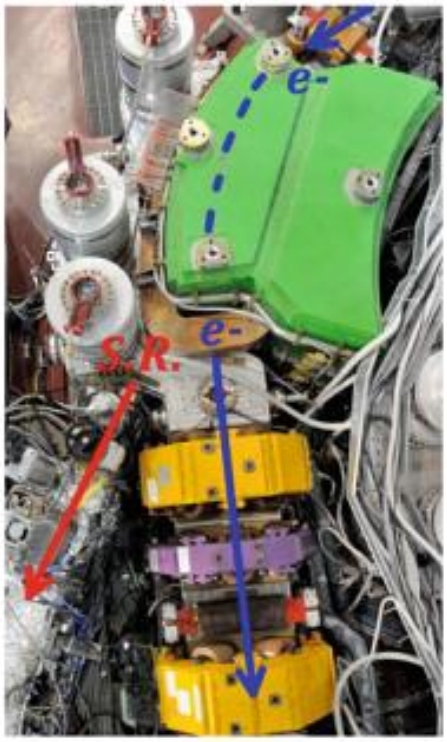

Fig. 1.5 One of the bending magnets of the INFN-LNF DAΦFNE storage ring and the initial part of a beamline collecting synchrotron radiation (*courtesy of V. Tullio*)

1.3 Synchrotron Radiation Properties

The main properties of the synchrotron radiation are the following

1. high intensity;
2. very broad and continuous spectral range from infrared up to the hard x-ray region;
3. natural narrow angular collimation;
4. high degree of polarization;
5. pulsed time structure;
6. high brightness of the source due to small cross section of the electron beam (see Fig. 1.4) and high degree of collimation of the radiation;
7. ultra-high vacuum environment and high beam stability;
8. all properties quantitatively evaluable.

All these properties depend on the characteristics of the storage ring and can be calculated by applying classical electrodynamics to the motion of relativistic charged particles. Some details on these important properties will be now introduced starting from the radiation emitted by bending magnets (BM) known as 'dipole radiation'. (see Fig. 1.5). In Chap. 2 these properties will be explained in more detail, in particular it will be shown that they have a relativistic origin.

1.4 Radiated Power and Time Structure

Accelerated charged particles emit electromagnetic radiation. In a storage ring, bending magnets keep electrons moving in a closed trajectory applying a magnetic field of fractions or few Tesla perpendicular to their velocity [5]. The acceleration of such particles is given by the Lorentz equation:

$$\frac{d\mathbf{p}}{dt} = e\left(\mathbf{E} + \frac{\mathbf{v} \times \mathbf{B}}{c}\right)$$

where $\mathbf{p}$, e and $\mathbf{v}$ are respectively the particle momentum, charge and velocity and $\mathbf{E}$ and $\mathbf{B}$ are the electric and magnetic fields.

The power radiated [1] by a relativistic electron forced to move along a circular orbit, with a radius of curvature, R, is given by the Schwinger's formula [5]:

$$P_e = \int\int P(\lambda, \psi) d\lambda d\psi = \frac{2}{3}\frac{e^2 c}{R^2}\left[\frac{E}{mc^2}\right]^4 \tag{1.1}$$

where λ is the wavelength of the emitted radiation, ψ is the azimuthal or vertical half-opening angle perpendicular to the orbital plane. $P(\lambda, \psi)$, the power radiated by an electron in a unit wavelength interval centered at λ and in a unit vertical angular aperture centered at ψ. E is the electron energy, m its mass, c is the speed of light and mc^2 is the electron rest mass energy (0.511 MeV). In (1.1), the dependence of the radiated power on E^4 must be noted; this implies that, to keep the radiated power at reasonable values, in order to increase the energy of the storage rings, it is necessary to increase also their radius. In the same equation it must be noted that, due to the dependence on m^{-4}, the radiation produced by proton accelerators is negligible.

The energy lost per turn by the charged particle, taking into account a revolution time, $2\pi R/c$, is given by:

$$\Delta E_e = \frac{4\pi}{3}\frac{e^2}{R}\left[\frac{E}{mc^2}\right]^4$$

In order to replenish the energy lost with the emission of radiation and keep the electrons at a constant energy, radio frequency (RF) cavities are used. In a RF cavity a longitudinal electric field accelerate the electrons. The RF fields have an accelerating effect only during one half of their period and a decelerating action during the other half; so the RF is effective in restoring the electron energy only for one half of the time. Additional considerations have to be performed, regarding the stability of the electron orbit. Let us suppose that at the time t_0 an electron passing through the RF finds exactly the electric field he needs to fully restore the energy lost during a turn. We will call this electron a "synchronous" electron (Fig. 1.6).

Synchronous electrons continue their motion along the ring returning in the RF again in time to regain the exact amount of energy lost along the circular path. So

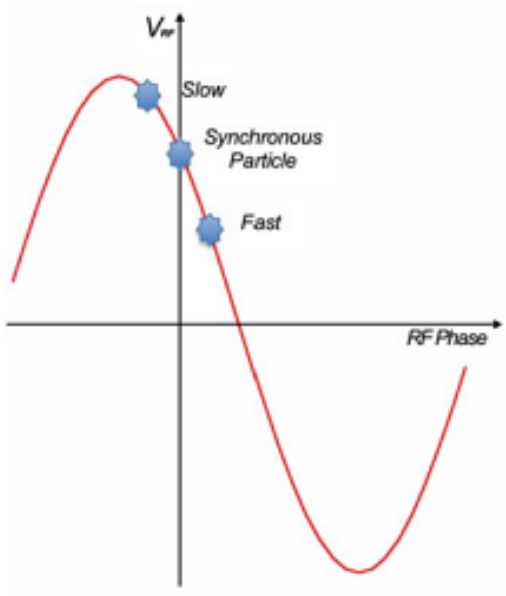

Fig. 1.6 Sinusoidal time dependence of the RF cavity voltage that effects energy restoration

the synchronous electrons are in a stable condition. Let us now consider electrons arriving in the RF a little bit later than the synchronous electrons. They are slower than the first ones, i.e. they have a lower energy. In order to restore the energy, they have to find an electric field higher than that found by the synchronous electrons otherwise they will continue to lose energy with respect to them. In the next turn they will arrive later, and after some turns they will enter the RF during the decelerating semi-period and will be lost. Vice versa electrons arriving before the synchronous ones must find a lower electric field, otherwise their energy will increase with respect to the synchronous electrons. These considerations show that only one half of the accelerating semi-period (i.e. one fourth of the period) is effective in maintaining the electrons on the orbit (Fig. 1.6).

The stability condition is effectively more strict, and only 5–10 % of the RF period is effective in restoring the electron energy. All the electrons, passing through the RF, not in phase with this 5–10 % effective time, do not follow the ideal circular orbit of the ring and therefore are lost. As a consequence the electrons in the storage ring are grouped in bunches with time lengths that are typically 5–10 % of the RF period. Also the radiation appears in pulses with the same time duration and separation (Fig. 1.7).

Along the storage ring many bunches can be distributed. The time interval between them is an integer multiple of the RF period (called harmonic number of the ring). The maximum separation between two pulses is obtained in the single bunch mode, i.e. when only one bunch in the full ring is present. In this case the time interval is equal to the period of revolution, typically of the order of microseconds. When more bunches are present the time interval is lower; the minimum possible time interval between bunches is equal to the RF period. The filling of bunches in a machine is a parameter that can be completely controlled; it is possible to choose how many and which bunches have in the ring. This flexibility is often used to relate to the photon

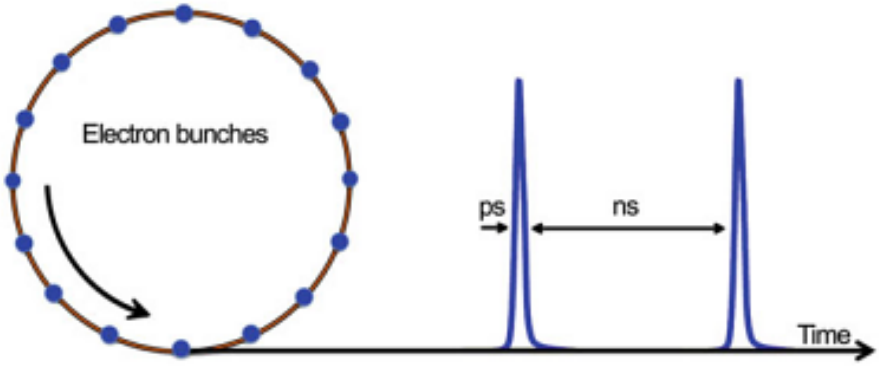

Fig. 1.7 Electron bunches moving in the storage ring produce radiation peaks having the same bunch length (ps) and separation (ns)

source different time dependence characteristics. The total current depends on the number of filled bunches. The current is lower when few bunches are filled, because the total amount of current that can be stored in a single bunch is limited.

Application to a third generation electron storage ring like the European Synchrotron Radiation Facillity (ESRF, Grenoble -FR).

- The energy of the electrons at ESRF is E = 6 GeV, it has a circumference (C) of 844 m, the frequency of the RF cavity is ν_{RF} = 355 MHz (8 MV RF accelerating voltage) and I_{max} = 200 mA is the maximum current.
- Single bunch mode: I = 20 mA

$$T_0 = C/c = 2.81\,\mu s$$

where T_0 represents the maximum time separation between bunches achievable only in single bunch mode.

- Uniform bunch mode: $I_{max} = 200\,\text{mA}$

$$T_{RF} = 1/\nu_{RF} = 2.82\,\text{ns}$$

where T_{RF} represents the minimum time separation between bunches achievable only in uniform bunch mode (corresponding to a separation of about 86 cm between them). The maximum number of bunches that can be stored depends on ν_{RF} and on $\nu_0 = (1/T_0)$:

$$N_{max} = \nu_{RF}/\nu_0 = 992.$$

The bunch lengths are normally of the order of *mm* corresponding to tens of *picoseconds*. At ESRF in uniform bunch mode the bunch length is of the order of 20 ps while in single bunch mode it is of the order of 73 ps.

1.5 Angular, Spectral and Intensity Distribution

In order to understand the angular and spectral distribution of the emitted radiation let us first remind the emission from a classical electron moving at a speed, v, much lower than the speed of light, c ($v \ll c$)(see Fig. 1.8).

In this case the emitted pattern is similar to that of an oscillating dipole with its maximum of intensity in the direction perpendicular to the acceleration and does not depend on the electron speed.

For a relativistic effect, when the speed of the emitting electrons increases to relativistic values ($v \approx c$) the radiation pattern is compressed into a narrow cone in the direction of motion, resulting into an emission tangential to the particle orbit. The vertical half-opening angle, ψ, is given by:

$$\psi \approx mc^2/E \approx \gamma^{-1}.$$

For electrons and positrons, in practical units:

$$\gamma = 1957E(\text{GeV})$$

so for a storage ring of energy $E = 1\,\text{GeV}$ it follows that $\psi \approx 0.5$ mrad $\approx 0.029°$: synchrotron radiation is highly collimated. This characteristic provides extremely high fluxes on very small areas also at distances of tens of meters from the storage ring.

In a bending magnet the horizontal collimation is lost because the electrons move along a circular orbit emitting the radiation along the tangent. The radiation is

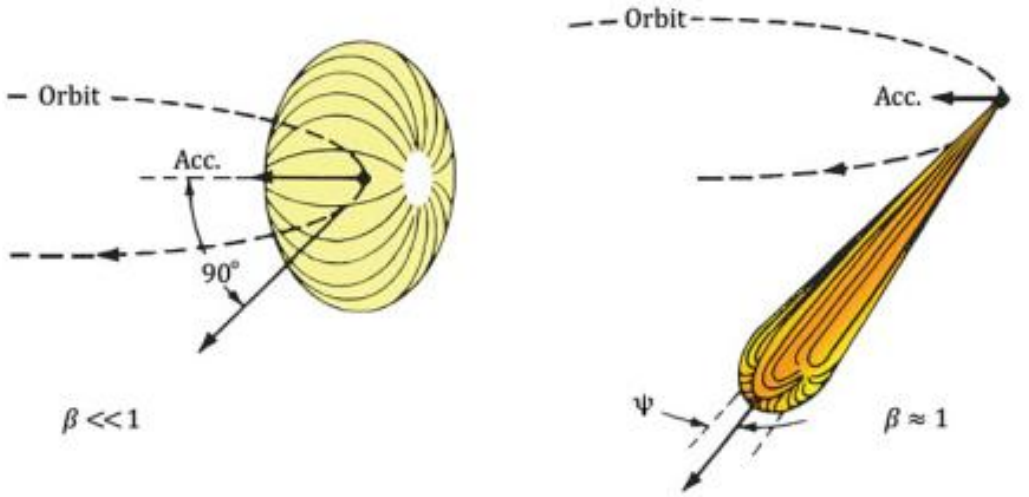

Fig. 1.8 Qualitative radiation patterns related to charged particles moving in a circular orbit. The dipole pattern achieved for slow particles (*left*) ($\beta = v/c << 1$) is distorted into a narrow cone when $\beta \approx 1$ (*right*) (the figure was redrawn: it is based on Fig. 1.1 of [6])

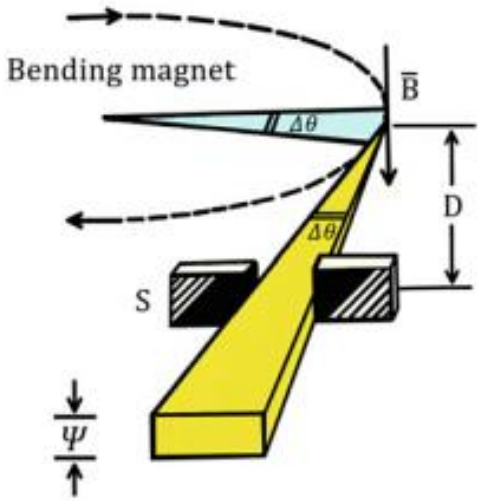

Fig. 1.9 Synchrotron radiation emitted by a relativistic electron travelling along a curved trajectory. The magnetic field is perpendicular to the electron orbit plane, Ψ is twice the natural opening angle in the vertical plane while $\Delta\theta$ is horizontal angular distribution, normally much bigger than Ψ limited in the figure by the horizontal slits, S

collected, for experiments, through a horizontal slit (S) of width, w, at a distance, D, from the electron orbit (see Fig. 1.9); this corresponds to an angular collection angle, $\Delta\theta = w/D >> \psi$.

It means that all the radiation emitted along an orbital arc, $\Delta\theta$, is collected and summed incoherently. For this reason the natural narrow collimation, ψ, is preserved only in the vertical direction, the direction perpendicular to the plane of the orbit as shown in Fig. 1.9. We anticipate here that using undulators as insertion devices the collimation can be kept in both directions.

The spectral distribution of the BM synchrotron radiation flux, is a continuous function, that extends from the x-ray to the infrared region (see Fig. 1.10) and is characterized by a critical wavelength, λ_c, given by:

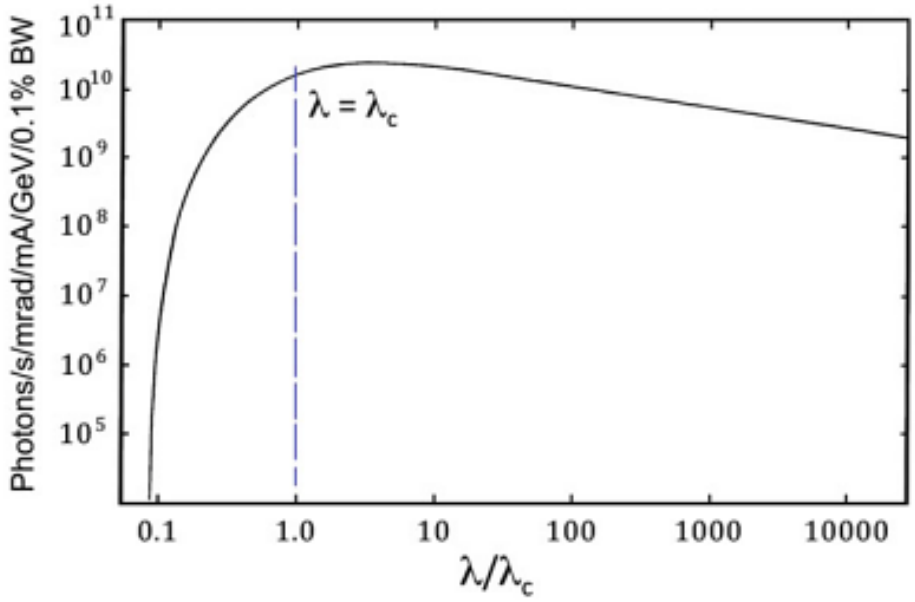

Fig. 1.10 Universal curve function of the spectral distribution of BM synchrotron radiation drawn as a function of λ_c/λ

$$\lambda_c = (4/3)\pi R\gamma^{-3} \text{ or in practical units } \lambda_c(\text{Å}) = 5.59\text{R(m)}\,\text{E}^{-3}\,\text{(GeV)}.$$

that depends only on the machine parameters γ and R. The critical wavelength, λ_c, represented by the discontinuous line in Fig. 1.10), divides the spectrum into two parts of equal radiated power: 50 % of the total power is radiated at wavelengths shorter than λ_c and 50 % at wavelengths longer than λ_c.

The physical origin of such broad distribution can be qualitatively understood. Let us consider to have a single electron moving in the storage ring and to record the emitted radiation using a point detector which looks tangentially at a specific point of the orbit (see Fig. 1.11). The detector will receive a short pulse of radiation every time the electron passes through that point of the orbit, i.e. at a frequency equal to the frequency of the period of motion $\omega = v/2\pi R$.

In the frequency domain the spectral distribution will be composed of the fundamental frequency and of its harmonics. At high frequency a cutoff will be present because the detector will receive the radiation emitted by the electron along the arc $2/\gamma$ and this originates a pulse of non zero duration, $\Delta\tau$, given by the difference between the time for the electron to travel along the arc and the time for the light to travel along the chord subtended by this arc (see Fig. 1.11):

$$\Delta\tau = \frac{R}{c}\left[\frac{1}{\gamma\beta} - 2sin\left(\frac{1}{2\gamma}\right)\right] \simeq \frac{R}{c\gamma^3}.$$

A light pulse of this duration has frequency components up to about:

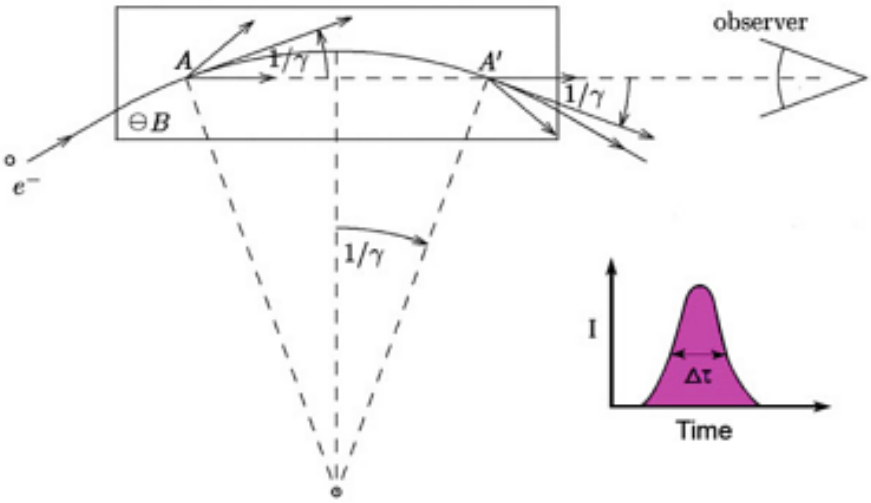

Fig. 1.11 Graphical view of the origin of the duration of the light pulse emitted by a bending magnet. The detector records the radiation emitted by the electron along the path from A to B (the figure was redrawn: it is based on Fig. II.2 of [7])

$$\omega_{cutoff} \approx \Delta\tau^{-1} = c\gamma^3/R$$

corresponding to a cutoff wavelength, $\lambda_{cutoff} = 2\pi R/\gamma^3 = 3/2\lambda_c$. Therefore, in principle, synchrotron radiation from one electron consists of a discrete spectrum of closely spaced lines up to ω_{cutoff}.

In practice, the spectral distribution coming from many electrons is continuous due to the statistical oscillations of the electrons around the main orbit, to the fluctuations in their kinetic energy and to the statistical nature of the emission itself: all effects that lead to a line broadening of each harmonic. This results in the continuous broad spectrum with the cutoff at $\lambda < \lambda_c$.

Quantitatively, the number of photons, $N(\lambda)$, emitted by a single electron in all the vertical angles, in a wavelength band of width $\Delta\lambda/\lambda$ centered at λ, while moving along an arc of length $R\Delta\theta$ is given by:

$$N(\lambda) = \frac{3^{1/2}}{2\pi}\frac{e^2}{hR}\gamma\, G_1 \frac{\Delta\lambda}{\lambda}\Delta\theta \tag{1.2}$$

where all quantities are expressed in CGS units. G_1, known as the *universal synchrotron radiation function* is the function plotted in Fig. 1.10.

In order to calculate the emission from a storage ring, it is necessary to multiply (1.2) by N_e the number of electrons in the storage ring given by:

$$N_e = I\,(2\pi R)/ec$$

where I is the electron current. This gives for $N\,(\lambda)$ the following equation:

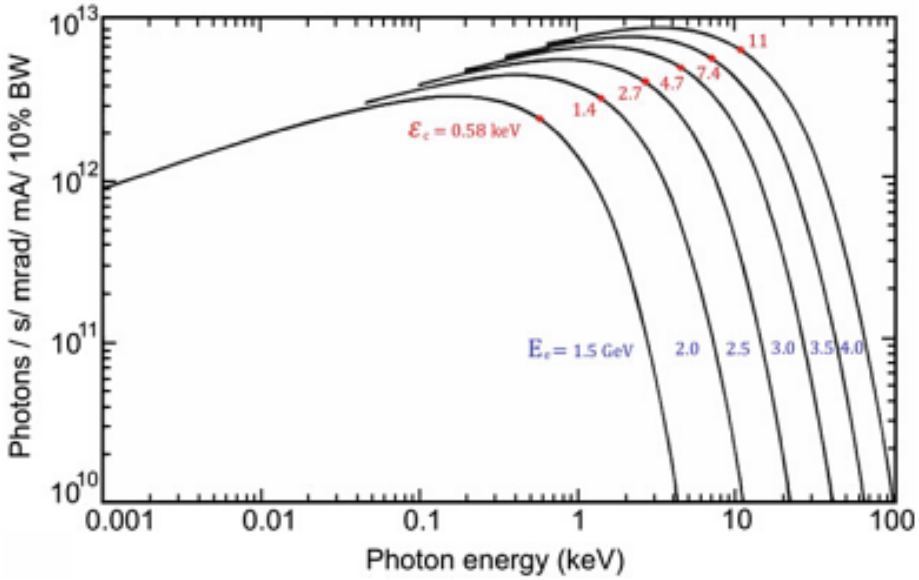

Fig. 1.12 Spectral distribution of synchrotron radiation as a function of the value of critical energy, ε_c, of the storage ring

$$N(\lambda) = 3^{1/2}\frac{e}{hc}\gamma I G_1 \frac{\Delta\lambda}{\lambda}\Delta\theta$$

that in practical units [8], assuming $\Delta\lambda/\lambda = 10^{-3}$ and $\Delta\theta = 1$ mrad can be written as:

$$N(\lambda) = 2.457 \times 10^{13} E[GeV] I[A] G_1 \left[\frac{photons}{\mathrm{s}\cdot 0.1\,\%\,\mathrm{BW}\cdot mrad\,\theta}\right]. \qquad (1.3)$$

The spectral distribution of the emitted photons, given by (1.3), is that shown in Fig. 1.10. For $\lambda \ll \lambda_c$ the spectral distribution falls off exponentially while for $\lambda \gg \lambda_c$ it decreases slowly, it is practically independent of the energy of the electrons and it is mainly determined by the current of the machine.

The photon flux is frequently expressed as a function of energy (Fig. 1.12); in order to do this, $y = \lambda_c/\lambda$ must be replaced by $y = \varepsilon/\varepsilon_c$ where $\varepsilon_c = hc/\lambda_c$ represents the critical energy given by:

$$\varepsilon_c = 3hc\gamma^3/(4\pi R)$$

or in practical units

$$\varepsilon_c(\mathrm{keV}) = 2.218 E^3(\mathrm{GeV})/R(m). \qquad (1.4)$$

As shown in Fig. 1.12, the maximum photon energy achievable with a storage ring is few times its critical energy, ε_c.

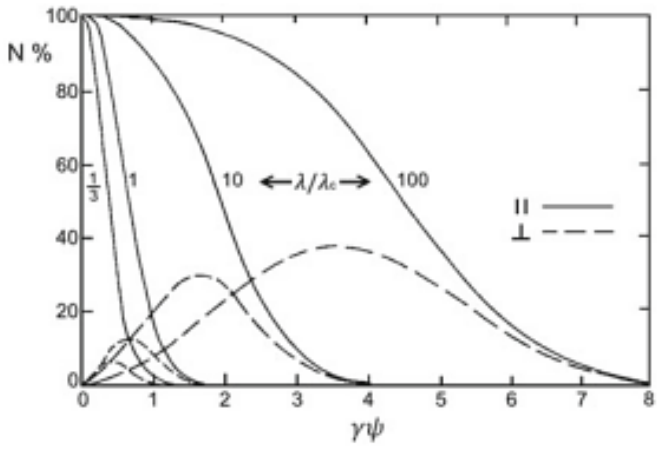

Fig. 1.13 Intensity of the parallel and perpendicular components of the photon flux as a function of $\gamma\psi$. The curves are reported for $\lambda/\lambda_c = 1/3, 1, 10$ and 100 and are normalized to the intensity at $\psi = 0$ (the figure is based on data of [9])

1.6 Polarization

The radiation emitted by a bending magnet is mostly linearly polarized. When observed in the horizontal plane, the electric field is parallel to the plane of the electron orbit (horizontal). Observing the radiation above and below this plane at finite vertical angles, a polarization component perpendicular to the plane of the electron orbit is present. In Fig. 1.13, the behavior of these two components as a function of $\gamma\psi$, is shown: it is clearly visible that the vertical opening angle, $\Delta\psi$, is approximately given by γ^{-1} ($\gamma\psi = 1$) when $\lambda \approx \lambda_c$. For $\lambda < \lambda_c$ the radiation fan is more collimated, while for $\lambda > \lambda_c$ it becomes wider.

The horizontal componnt has its maximum roughly at angles at which the intensity of the vertical component is 1/2 of its maximum.

Because of the presence of a horizontal and a vertical component, it is useful to define the degree of linear polarization, P_{Linear}, as [1]:

$$P_{Linear} = \frac{I_{//} - I_{\perp}}{I_{//} + I_{\perp}}.$$

In the orbital plane, ($\psi = 0$), P is equal to 1, i.e. the light is 100 % linearly polarized. When the observation is off axis the linear polarisation decreases as a function of $\gamma\psi$. The integration over all wavelengths gives:

$$I_{//} = (7/8)I_{total} \qquad I_{\perp} = (1/8)I_{total}$$

that means a linear polarisation degree of about 75 %.

Above and below the plane there is a constant phase difference of $+\pi/2$ and $-\pi/2$ between the parallel and perpendicular components of the electric field. Therefore the radiation is respectively elliptically right and left polarized. The degree of circular polarisation, P_C, defined as:

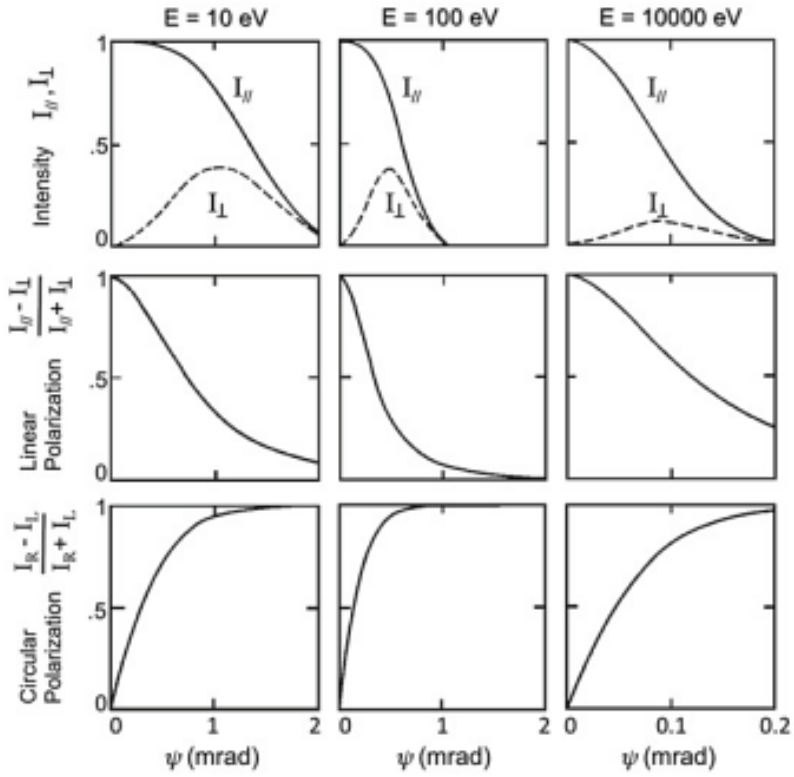

Fig. 1.14 Intensity distribution of the parallel and perpendicular components of the radiation as a function of ψ at three different photon energies, for a storage ring with $E = 3.5\,\text{GeV}$, $R = 12.12\,\text{m}$; the critical energy is 7.8 keV and $1/\gamma$ is 0.146. The behaviour of the *linear* and *circular* degrees of polarisation are also shown (the figure was redrawn: it is based on Fig. 1.8 of [1])

$$P_C = \frac{I_R - I_L}{I_R + I_L} = \frac{\pm 2\sqrt{(I_{//} I_{\perp})}}{I_{//} + I_{\perp}}$$

where I_R and I_L are the intensities of the right and left polarized light and the sign, $\pm$, corresponds to positive or negative values of ψ, is shown in Fig. 1.14, and compared with the degree of linear polarisation.

The vertical angular dependence of the SR beam on the vertical angle ψ can be well approximated by a Gaussian function $1/(2\pi\sigma_R^2)^{0.5} \exp(-\psi^2/2\sigma_R^2)$ [9]; σ_R, in the range $0.2 < \lambda/\lambda_c) < 100$, is approximately given by:

$$\sigma_R = \frac{0.565}{\gamma}\left[\frac{\lambda}{\lambda_c}\right]^{0.425}$$

where σ_R is expressed in radians. The FWHM ($2.35\sigma_R$) of the angular distribution in practical units is given by:

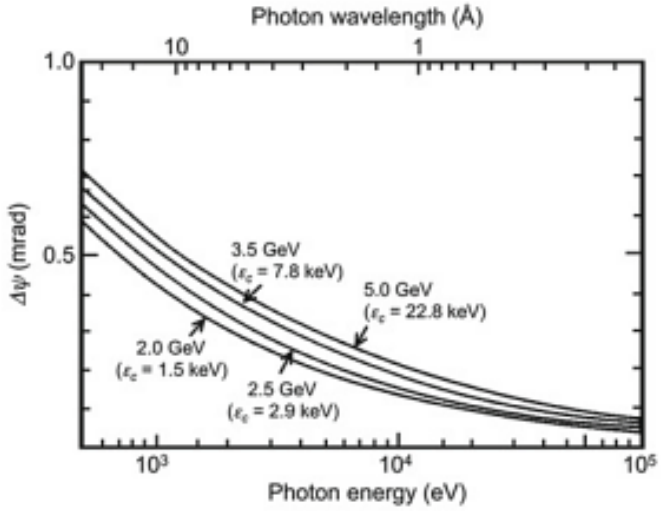

Fig. 1.15 Values of the angular width $\Delta\psi$ plotted a function of photon energy for different values of the electron energy and of the critical energy (the figure was redrawn from Fig. 1.5 of [10])

$$\Delta\psi\,(FWHM) = 2.35 \cdot \sigma_R = \frac{0.682}{E(GeV)}\left[\frac{\lambda}{\lambda_c}\right]^{0.425}$$

In Fig. 1.15, $\Delta\psi$ is shown as a function of the photon wavelength/energy and of the energy of the storage ring.

Normally, σ_R, that represents the standard deviation of the vertical angular distribution of the SR beam, includes also a contribution due to the divergence of the electron beam negligible for storage rings having small electron beam divergence and dimension.

1.7 Spectral Brightness and Emittance

An useful quantity for experiments which do not use focussing optics, is the photon flux per solid angle, because from it the flux on the sample can be easily evaluated using simple geometrical considerations. This quantity, defined as the number of photons emitted per second, in a spectral bandwidth $\Delta E/E = 0.1\,\%$, into a unit solid angle, is given by:

$$N = 1.327 \times 10^{13} E^2[\mathrm{GeV}]\, I\,[\mathrm{A}] H_2(\mathrm{y})$$

where H_2 is (like G_1) a dimensionless function of $y = \varepsilon/\varepsilon_c$, whose behaviour is reported in Fig. 1.17. It has a broad maximum around ε_c, decreases as $(\varepsilon/\varepsilon_c)^{2/3}$ for $\varepsilon/\varepsilon_c \ll 1$ and as $[\varepsilon/\varepsilon_c \exp(-\varepsilon/\varepsilon_c)]$ for $\varepsilon/\varepsilon_c \gg 1$ (Fig. 1.16).

When focussing optics are used, the relevant quantity is the photon intensity that can be focused into a specific area; at this purpose the *spectral brightness* of the source must be calculated. It is defined as the number of photons emitted per

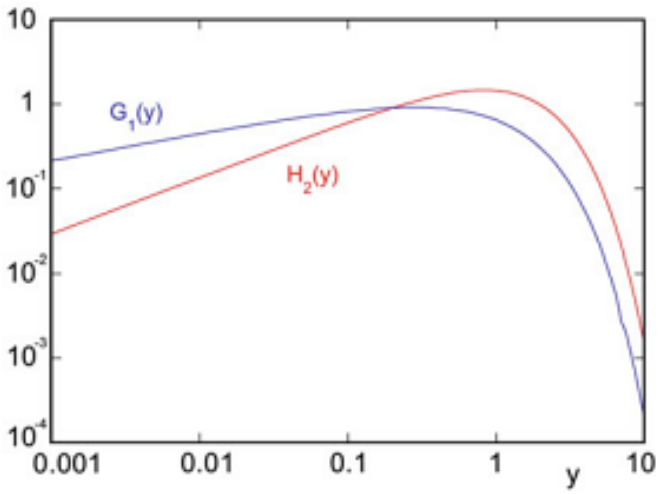

Fig. 1.16 Comparison of the spectral dependence of the $G_1(y)$ and of the $H_2(y)$ functions

second, in a spectral bandwidth $\Delta E/E = 0.1\,\%$ in an unit source area and per unit of solid angle. As well known due to the Liouville's theorem, focussing preserves the brightness, i.e. the brightness of the source is equal to the brightness of the beam when focussed on the sample. The brightness is determined by the size of the source, that is given by the size of the electron beam and by the angular spread of the radiation, given by the convolution of the angular distribution of synchrotron radiation, $\Delta\psi$, with the angular divergence of the electron beam. Therefore the characteristics of the electron beam source are essential in order to determine the brightness of the photon source. In a storage ring the product of the electron beam transverse size and angular divergence is a constant along the ring and is called emittance. Although the electron beam transverse size and angular divergence vary around the ring, their product or emittance is a constant. There is a horizontal and a vertical emittance. The horizontal emittance is measured in nanometer-radians (nm-rad).The vertical emittance is normally a few percent of the horizontal one. In order to get high brightness, small emittance machines must be used.

Brightness is the main figure of merit of synchrotron radiation sources and its huge increase, shown in Fig. 1.4, was obtained thanks to the designing of low emittance machines, like the European Synchrotron Radiation Facility (ESRF), that minimize the source size and the beam divergence.

1.8 Insertion Devices

Insertion devices (ID) are periodic magnetic structures installed in the straight sections of storage rings. Passing through such alternating magnetic field structures, electrons oscillate perpendicularly to the direction of their motion and therefore emit synchrotron radiation during each individual wiggle. The primary effects of the IDs are:

(1) the shift of the critical energy to higher values due to the smaller bending radius with respect to the bending magnets;

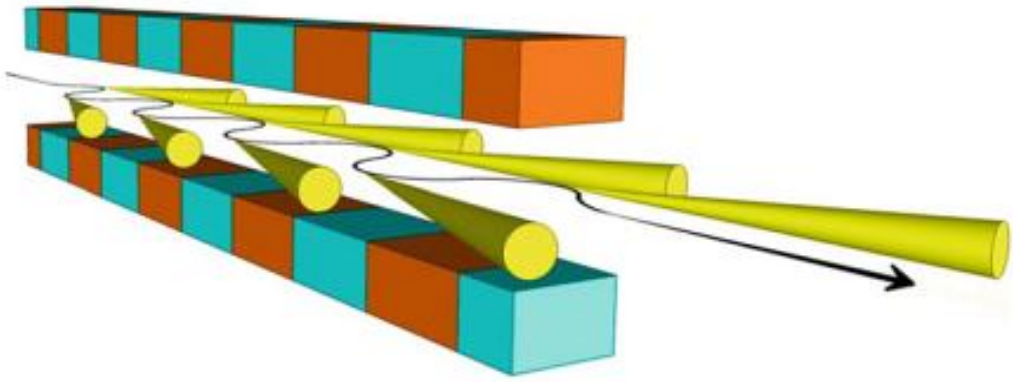

Fig. 1.17 Artistic view of the radiation beam emission from a multipole wiggler magnetic structure *(courtesy of V. Tullio INFN-LNF)*

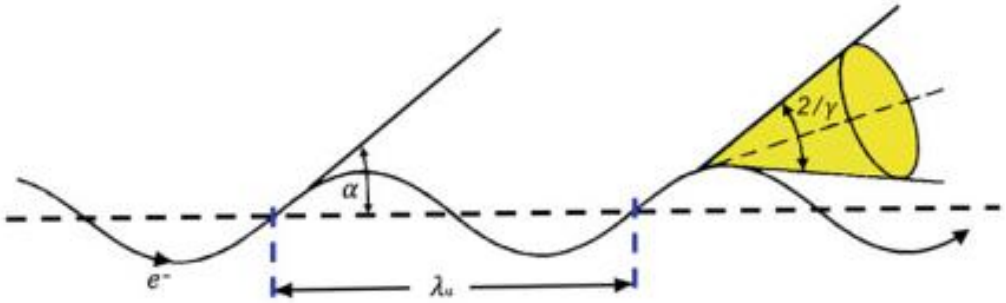

Fig. 1.18 Schematic view of the 'wiggler' regime, where λ_u represents the period of the oscillations

(2) the increase of the intensity of the radiation by a factor related to the number of wiggles induced by the many poles of the magnetic structure;
(3) the relevant increase of the spectral brightness.

Insertion devices are of two kinds: wigglers and undulators. Inside both these devices the electron beam is periodically deflected but outside no deflection or displacement of the electron beam occurs (Fig. 1.17).

A wiggler is a multipole magnet made up of a periodic series of magnets (N periods of length λ_u, the overall length being $L = N\lambda_u$), whose magnetic field forces the electrons to wiggle around the straight path (Fig. 1.18).

The alternating magnetic field is normally applied in the vertical direction so the sinusoidal trajectory of the electron beam lies in the horizontal plane. Electrons follow in this way a curved trajectory with a smaller local radius of curvature with respect to the one of the dipole-bending magnet, because in a wiggler, magnetic fields, higher than in a bending magnet can be used.

Using the value of the instantaneous radius of curvature of the electron trajectory, R(m):

$$R(\mathrm{m}) = 3.34E(\mathrm{GeV})/B(\mathrm{T})$$

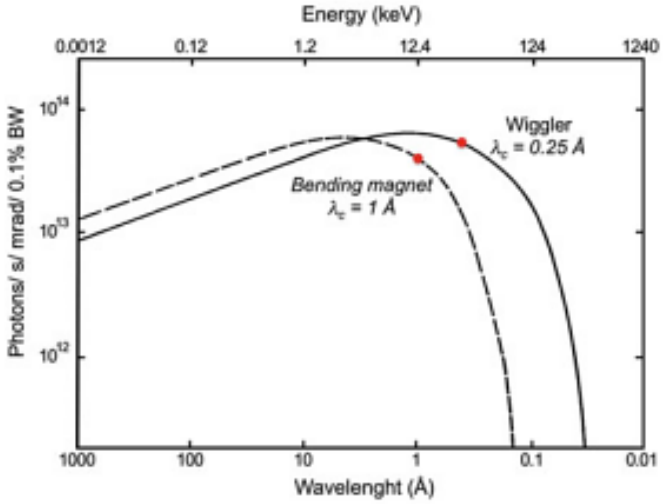

Fig. 1.19 Comparison between the spectral flux from a bending magnet (—) (B = 0.74 T) and from a wiggler (wavelength shifter: N = 1, B = 3.0 T))

where B is the magnetic field strength given in Tesla and using (1.4) the critical energy, ε_c, can be expressed as:

$$\varepsilon_c(\text{keV}) = 0.665\, E^2(\text{GeV})B(\text{T}).$$

The use of higher magnetic fields increases the critical energy with respect to the values achievable with bending magnets and extends the spectral range of a storage ring towards higher energies (Fig. 1.19).

The radiation observed is the incoherent sum of the radiation emitted by each individual pole. Therefore the overall characteristics of the beam are the same as those of a bending magnet with the same magnetic field but with an intensity enhanced by the factor N, the number of poles.

The total power generated by a wiggler is given, in practical units, by the equation:

$$P_T[\text{kW}] = 0.633E^2[\text{GeV}]B^2[\text{T}]L[\text{m}]I[\text{A}]$$

where B and L are the maximum magnetic field and length of the device.

In order to introduce undulators and clarify their difference with respect to wigglers, we make use of the dimensionless parameter K. It is given by the ratio between the wiggling angle of the trajectory, α, and the natural angular aperture of synchrotron radiation, $1/\gamma$, (Fig. 1.18) i.e.

$$K = \alpha\gamma.$$

For an electron moving in a sinusoidal magnetic field, it is easy to show that K is given by:

$$K = \frac{e}{2\pi mc}\lambda_u B = 0.934\,\lambda_u\,[\text{cm}]B[T]$$

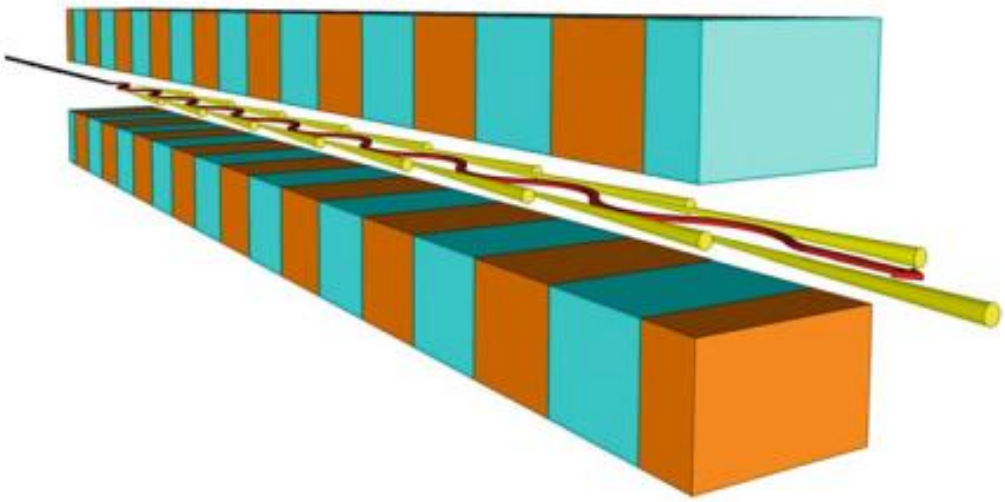

Fig. 1.20 Artistic view of the radiation beam emission from a multipole undulator magnetic structure (*courtesy of V. Tullio INFN-LNF*)

where, λ_u , is the period of the device. In a wiggler the transverse oscillations of the electrons are very large and the angular deviations, α, (Fig. 1.18) much wider than the natural opening angle $\psi = \gamma^{-1}$, therefore K >> 1. In these large K devices, the interference effects between the emission from the different poles can be neglected and the overall intensity is obtained by summing the contribution of the individual poles.

An undulator is very similar to a wiggler, but its K value is less than 1, that means, that the wiggling angle α is smaller than, or close to, the photon natural emission angle γ^{-1} (Fig. 1.20).

In this case interference occurs between the radiation emitted by electrons at different points along the trajectory. Considering the phase differences between the photons emitted at different points along the sinusoidal orbit, it is easy to show that observing the radiation in a direction forming an angle θ with the axis of the undulator, constructive interference occurs at the wavelength, λ:

$$\lambda = \frac{\lambda_u}{2\gamma^2}\left(1 + \frac{K^2}{2} + \gamma^2\theta^2\right). \tag{1.5}$$

In addition to the fundamental wavelength, also higher harmonics of shorter wavelength, $\lambda_n = \lambda/n$, are emitted (1.21). Their number and intensity increases with K; on the axis ($\theta = 0$) only odd harmonics are emitted.

The dependence of λ on K^2 that is on B^2 (1.5) is of extreme importance, because allows to vary the energy of photon emission. In the insertion devices the magnetic gap is the distance between the upper and lower arrays of magnets (Fig. 1.22) and in some ID it is fixed while in other it can change. The widening or shortening of the

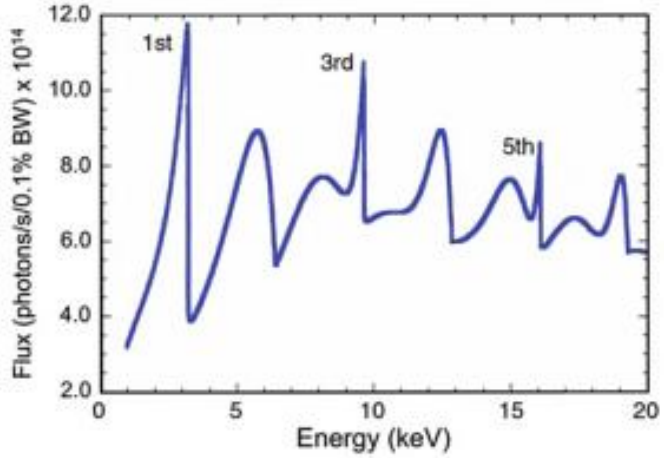

Fig. 1.21 Calculated flux spectrum of the APS (Advanced Photon Source (7 GeV)- Argonne (Illinois)) undulator A, a planar device (L = 2.4 m, N = 72) optimized to generate x-ray photons in a wide energy range, using the first, third and fifth radiation harmonics (*sharp peaks*), with I = 100 mA, K = 2.6 giving $E_1 = 3.21$ keV and no slits (the figure was redrawn: it is based on data of [11])

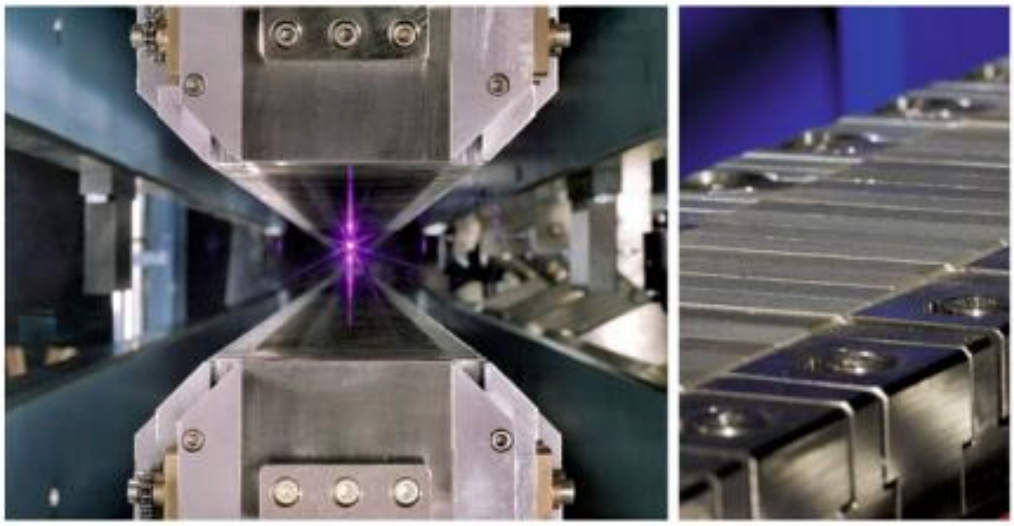

Fig. 1.22 *Left panel* Looking head on into the upper and lower rows of magnets (*jaws*) in an undulator. The adjustable vertical distance (*gap*) between the jaws determines the emitted wavelength. A laser was used to simulate the burst of light produced (*courtesy of Advanced Light Source*). *Right panel* Lower row of magnets of one of the SPARC undulators (*courtesy of SPARC_ LAB group INFN-LNF*)

gap distance in an undulator has an inverse effect on the amplitude of the magnetic field and is routinely used to change λ.

In an undulator, the amplitudes of the fields radiated by each individual period of the undulator add up coherently, so the intensity increases with N^2 while it increases only as 2N in a wiggler.

Each harmonic has a limited wavelength bandwidth approximately given by:

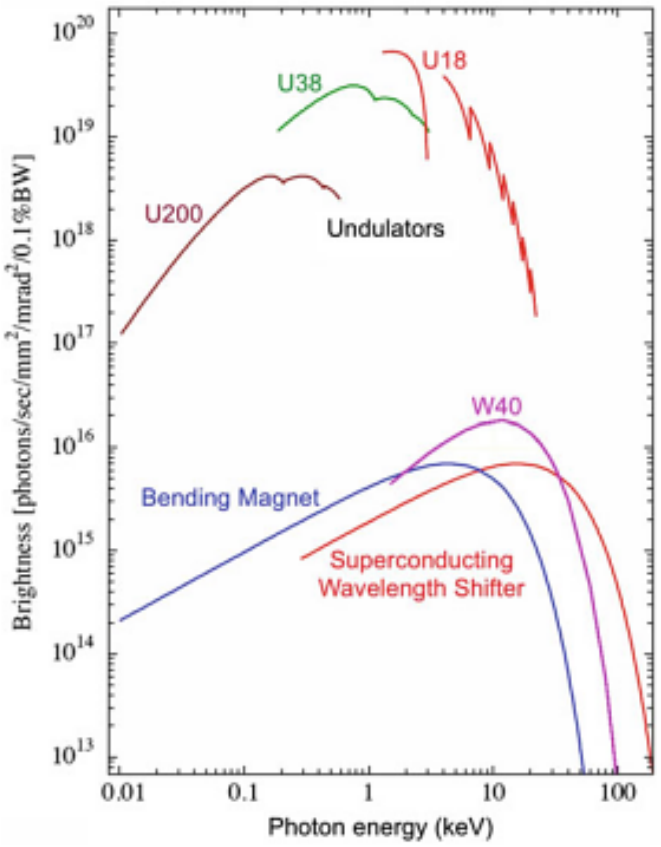

Fig. 1.23 Calculated brightness of beams emitted by undulators (200 mm (L = 10 m), 38 mm (L = 4 m) and 18 mm (L = 2 m) periods), wigglers (wavelength shifter and 40 mm (L = 2 m) period) and bending magnets for a 2.4 GeV storage ring with 400 mA circulating current (the figure was redrawn: it is based on data of [12])

$$\Delta\lambda/\lambda \;=\; 1/(nN)$$

Values of 10^{-2} can be easily achieved on the fundamental. Note that the bandwidth decreases with the number, N, of periods of the undulator and with the harmonic number, n.

The angular distribution, of the n-th harmonic is concentrated in a narrow cone in both the horizontal and vertical directions (Fig. 1.20) whose half width is given by:

$$\sigma = \sqrt{\frac{3}{4\pi}\frac{1+(K^2/2)}{\gamma^2 nN}} \approx \frac{1}{\gamma}\frac{1}{\sqrt{nN}}$$

so it is always lower than the natural emission cone, $1/\gamma$ of a bending magnet and decreases as the square root of the number of poles and of the harmonic number.

This very narrow angular distribution together with the N^2 dependence of the intensity radiated in the 'undulator' regime explain why the spectral brightness achievable with undulators exceeds by several order of magnitude that of bending magnets and of wigglers (Fig. 1.23).

We underline here that the observed properties of the photon beam are determined also by the electron beam emittance; while first and second-generation rings have an horizontal emittance of the order of 100–200 nm-rad, third generation ones are

in the 3–25 nm-rad range. Such low emittance values made possible to achieve the incredible brightness of the third generation synchrotron radiation facilities. However the increase in photon beam brightness as a function of the emittance decrease has a limit given by diffraction effects. The diffraction limited emittance or lowest useful emittance to produce high brightness photons of a given wavelength is $\lambda/4\pi$: for a photon energy of 1 keV the diffraction limited electron beam emittance is of the order of 0.1 nm-rad.

IDs are normally classified also as a function of the different technologies used to generate the magnetic fields, that include the use of electromagnets at room temperature (conventional iron and coil magnets) or superconducting (superconducting coils with or without iron) and the use of permanent magnets (NdFeB and SmCo). At room temperature if high photon energies are required, the highest magnetic field at the shortest possible period is necessary and for this reason normally permanent magnets are used (B_{max} = 3–4 T): electromagnets are an economical choice but produce smaller magnetic fields (factor 2–5). To overcome the problem related to the maximum achievable magnetic field, superconducting electromagnets can be used (B_{max} = 10–12 T). Operating at the liquid He temperature (4 K) superconducting IDs are more expensive to build and operate than permanent magnets but represent the most important and cheap solution to achieve high critical energies with a high magnetic field rather than increasing the whole storage ring energy. Nowadays most of the IDs, operating with a periodic vertical field, are realized using permanent magnets. In order to perform very specific studies like the ones needing circular polarization, complex IDs, like helical undulators can be also designed and built. Helical undulators generate helical magnetic fields that force electrons to move along spirals and emit circularly polarized radiation. In practice the use of the insertion devices in the third generation facilities has opened also the possibility to perform a quite large number of experiments that were quite impossible or difficult to realize in the past.

Acknowledgments The authors are very grateful to Mr. Vinicio Tullio for his help in the realization of many figures of this lecture.

Appendix: Basic Synchrotron Radiation Equations

Synoptic overview of some basic synchrotron radiation equations:

- Power radiated by a relativistic electron along a circular orbit (radius R):

$$P_e = \frac{2}{3}\frac{e^2 c}{R^2}\left[\frac{E}{mc^2}\right]^4$$

  or in practical units:

$$P_e(kW) = 6.76\times 10^{-10} E^4(GeV) R^{-2}(m).$$

  and in practical units the power radiated in a storage ring:

$$P(kW) = 88.47 E^4(GeV) I(A) R^{-1}(m).$$

- Vertical half-opening angle, ψ:

$$\psi \approx mc^2/E \approx \gamma^{-1}$$

  where for electrons and positrons, in practical units:

$$\gamma = 1957\, E\,(\mathrm{GeV}).$$

- The critical wavelength, λ_c:

$$\lambda_c = (4/3)\pi R \gamma^{-3}$$

  or in practical units:

$$\lambda_c(\text{Å}) = 5.59\mathrm{R(m)E^{-3}(GeV)}.$$

- Critical energy, ε_c in practical units:

$$\varepsilon_c(\mathrm{keV}) = 2.218\mathrm{E}^3(\mathrm{GeV})\mathrm{R}^{-1}(\mathrm{m}).$$

- Bending radius, R:

$$R(\mathrm{m}) = 3.34\mathrm{E(GeV)B}^{-1}(\mathrm{T}).$$

References

1. E.E. Koch, D.E. Eastman, Y. Farges, Synchrotron radiation—a powerful tool in science, in *Handbook of Synchrotron Radiation*, ed. by E.E. Koch (North-Holland Publishing Company, Amsterdam, 1983), pp. 1–63
2. Lightsources of the World. http://www.lightsources.org/regions
3. D.M. Mills et al., Report of the Working Group on Synchrotron Radiation Nomenclature brightness, spectral brightness or brilliance? J. Synchrotron Rad. **12**, 385 (2005)
4. H. Winick, Synchrotron radiation sources—present capabilities and future directions. J. Synchrotron Rad. **5**, 168–175 (1998)
5. J. Schwinger, On the classical radiation of accelerated electrons. Phys. Rev. **75**, 1912–1925 (1949)
6. D.H. Tomboulian, P.L. Hartman, Spectral and angular distribution of ultraviolet radiation from the 300-mev cornell synchrotron. Phys. Rev. **102**, 1423–1447 (1956)
7. D. Raoux, in *Introduction to Synchrotron Radiation and to the Physics of Storage Rings*, ed. by J. Baruchel et al. Neutron and Synchrotron Radiation for Condensed Matter Studies (Les Editions de Physique, Springer, 1993), pp. 37–78
8. P.J. Duke, *Synchrotron Radiation Sources*, ed. by A.G. Michette, C.J. Buckley. X- Ray Science and Technology (Institute of Physics Publishing, London, 1993), pp. 64–109
9. G.K. Green, *Spectra and Optics of Synchrotron Radiation, Report BNL 50522: Particle Accelerators and High-Voltage Machine-TID 4500* (Brookhaven National Lab, Upton, 1976), pp. 1–63
10. G. Materlik, in *Properties of Synchrotron Radiation*, ed. by H.B. Stuhrmann. Uses of Synchrotron Radiation in Biology (Academic Press Inc., London, 1982), pp. 1–21
11. W.-K. Lee, P. Fernandez, D.M. Mills, in *X-Ray Crystal Optics*, ed. by H. Onuki, P. Elleaume. Undulators, Wigglers and Their Applications (Taylor & Francis, London, 2003), pp. 369–420
12. M. Boge et al., The Swiss Light Source Accelerator Complex: An Overview. http://accelconf.web.cern.ch/Accelconf/e98/PAPERS/MOP28G.PDF